



## How Does Image Complexity Affect the Accuracy of an Interactive Image Segmentation Algorithm?

Kok Luong Goh<sup>1,2,\*</sup>, Soo See Chai<sup>3</sup>, Muzaffar Hamzah<sup>2</sup>, Emily Sing Kiang Siew<sup>1</sup>

<sup>1</sup> Faculty of Computing and Software Engineering, i-CATS University College, Jalan Stampin Timur, 93350 Kuching, Sarawak, Malaysia

<sup>2</sup> Faculty of Computing & Informatics, University Malaysia Sabah, 88400 Kota Kinabalu, Sabah, Malaysia

<sup>3</sup> Faculty of Computer Science & Information Technology, University Malaysia Sarawak, Kota Samarahan, 94300 Sarawak, Malaysia

### ARTICLE INFO

#### Article history:

Received 26 September 2023

Received in revised form 7 May 2024

Accepted 23 May 2024

Available online 20 June 2024

### ABSTRACT

This study investigates the impact of image complexity on the accuracy of interactive image segmentation algorithms. Image complexity plays a crucial role in segmentation performance, yet previous studies have primarily relied on subjective methods, leaving a gap in understanding how objective measures impact accuracy. The purpose of this research is to explore the relationship between image complexity and segmentation performance and to propose an adaptive approach for improving accuracy based on complexity measures. The study utilizes objective measures, namely entropy and fractal dimension, to quantify image complexity. An interactive image segmentation algorithm is employed, with a bounding box as the background and strokes as the foreground annotations. The number of strokes is dynamically adjusted based on complexity measures, ensuring a tailored segmentation approach. Comparative evaluations are conducted to assess the effectiveness of dynamic and fixed stroke allocation strategies. The principal results reveal a significant influence of image complexity on segmentation accuracy. The dynamic stroke allocation strategy outperforms fixed allocation, highlighting the importance of adapting to complexity. Moreover, the optimal combination of strokes and superpixel sizes is explored, providing valuable insights for practitioners. The findings emphasize the need to consider image complexity in segmentation algorithms to achieve accurate results. In conclusion, this study contributes to the understanding of the relationship between image complexity and interactive image segmentation. By introducing a dynamic stroke allocation approach and evaluating different configurations, the research provides insights into optimizing accuracy based on image complexity. The adaptive strategy improves segmentation performance and guides the development of robust algorithms. Future research can further refine the adaptive approach, explore additional complexity measures, and incorporate advanced machine learning techniques to enhance interactive image segmentation. Overall, this study advances the field by highlighting the importance of image complexity, providing guidance for practitioners, and paving the way for more efficient segmentation algorithms.

#### Keywords:

Interactive image segmentation; Image complexity; Superpixel

\* Corresponding author.

E-mail address: [klgoh@icats.edu.my](mailto:klgoh@icats.edu.my)

<https://doi.org/10.37934/araset.47.1.94104>

## 1. Introduction

Segmenting an image into discrete regions that each represent a unique object or feature is known as image segmentation. The purpose of image segmentation is to reduce the complexity of an image's representation so that it can be more readily analysed. Applications ranging from autonomous vehicles to medical imaging [1] and object recognition could benefit greatly from this. There are manual, semi-automated, and automated approaches to segmenting images.

First, there is manual image segmentation, which entails identifying and highlighting objects or regions of interest in an image, and then manually outlining or tracing their boundaries. This may be laborious and arbitrary, but it may also yield excellent results.

Second, there is semi-automated image segmentation, which makes use of tools and algorithms to aid in the segmentation process but still necessitates human involvement. One such technique is known as "interactive image segmentation," in which the user actively participates in the algorithm's decision-making by tweaking its parameters or providing other input.

Third, there is automated image segmentation, in which algorithms are used to separate out different parts of an image without any human intervention. These algorithms may make use of any number of different methods, including but not limited to thresholding, clustering, region growing, graph-based techniques, deep learning, etc. While automated image segmentation may be more time-efficient than manual or semi-automated approaches, the quality of the resulting segments may suffer, especially when working with images that are particularly complex or diverse. Interactive image segmentation is a type of semi-automated image segmentation where a user interacts with the algorithm to guide the segmentation process. The user provides input to the algorithm, such as outlining or tracing the boundaries of objects or regions of interest or adjusting parameters that influence the segmentation results. While various image segmentation types exist, understanding the impact of image complexity on their performance is crucial.

Understanding image complexity is crucial in various applications. It enables determining the compression level and bandwidth allocation, as low-complexity images can be more easily compressed and require less bandwidth compared to high-complexity images [2]. The effects of complex and simple images on interactive image segmentation have been addressed in previous studies [3]. However, defining an image's complexity is not a straightforward task, and various approaches have been proposed to estimate it.

To determine the complexity of an image, algorithms have been categorized into subjective and objective methods. Subjective methods rely on human perception, where observers rate image complexity on a scale or perform tasks, such as counting objects, using the completion time as a complexity measure. Objective methods employ mathematical or computational measures. These can include quantifying entropy, counting edges or edges per unit area, using fractal dimension to measure object complexity, or leveraging machine learning models to predict image complexity.

In the literature, several types of complex images have been identified. These include images with similar foreground and background colours, images with complex contents, and images with noise [4]. Additionally, a recent study introduced a new category of complex images, wherein the object of interest is overlapped with other similar objects [5].

To deepen our understanding of the relationship between image complexity and the performance of interactive image segmentation, our study takes a novel approach by leveraging objective measures of complexity. While previous studies have made significant strides in evaluating image complexity, they have predominantly relied on subjective methods, leaving a gap in our knowledge regarding the impact of objective measures on the accuracy of interactive image segmentation.

Existing research has examined various factors such as the number of strokes, superpixel sizes [6,7], and different superpixel algorithms[8] on complex images. However, it is worth noting that previous studies often determined the complexity of images using subjective methods. In our study, we aim to address this limitation by applying objective measures to determine the complexity of the images.

By incorporating objective measures of complexity, we aim to provide a more comprehensive understanding of how image complexity influences the performance of interactive image segmentation algorithms. This approach allows us to bridge the gap between subjective perceptions and quantifiable measures, contributing to a more robust evaluation of the segmentation accuracy. The next section will provide an in-depth overview of our methodology, explaining how we measure image complexity, apply the interactive image segmentation algorithm, and evaluate segmentation accuracy.

## 2. Methodology

The methodology section provides a detailed blueprint of our study, illustrating the intricate processes that were taken. It systematically delineates our approach, starting from the measurement of image complexity, followed by the determination of user input based on this complexity, the generation of superpixels, the application of the interactive image segmentation algorithm, and finally, the evaluation of the accuracy of the resulting segmentations (Figure 1). The following paragraph goes deeper into each component utilized in this methodology, providing a granular view of our research design and execution.

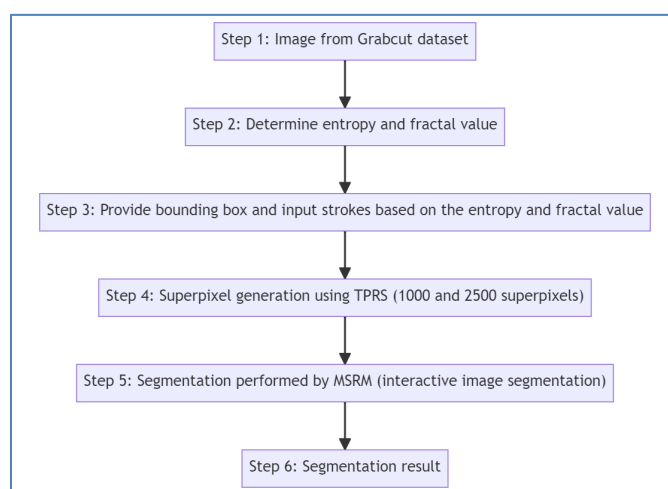


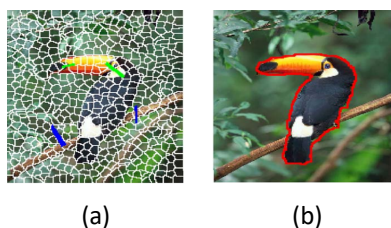
**Fig. 1.** Process flow of the research method

In order to conduct our experiment and evaluate the performance of the interactive image segmentation algorithm, we utilized a carefully curated dataset that encompasses a diverse range of images.

Grabcut dataset [9] consists of a collection of images (50 images) that are typically used for evaluating the performance of interactive image segmentation algorithms. The dataset includes various types of images, such as natural scenes, objects, and people, with different levels of complexity and diversity. The discussion of the interactive image segmentation that used in this study will be presented in the next section.

Maximal Similarity-based Region Merging (MSRM) [10] is based on region merging. The image is first converted into superpixels using mean shift segmentation. The contour of the object is then

extracted based on the labelling of non-marked regions as region of interest or background. Figure 2(a) shows the superpixels of the image with strokes on the background and object of interest, and 2(b) shows the segmentation result.



(a) (b)  
**Fig. 2.** The algorithm's segmentation process: (a) Superpixel strokes entered by users (b): the segmentation outcome

To enable efficient and effective user interaction in the image segmentation process, we employed the concept of superpixels [11]. By grouping pixels into perceptually meaningful regions, superpixels offer a more structured representation of the image, allowing users to interact with larger coherent units rather than individual pixels. In this study, topology preserved regular superpixel (TPRS) [3] will be used in this study. It is a path-based method that partitions an image into superpixels by connecting seed points via pixel path. It begins by arranging initial seeds on a lattice grid and associating them with appropriate pixels on the boundary map. It then relocates each seed to the pixel with the highest locally maximal edge magnitudes, taking into account both the distance term and the probability term. Finally, it finds the local optimal path between vertical and horizontal seed pairs. In the previous study [7], the MSRM was able to produce an ideal segmentation result with a bounding box with three strokes by employing superpixel sizes of 1000 and 2500. As a result, this configuration will be employed in this study.

To quantify image complexity and examine its influence on segmentation accuracy, we employed objective measures, specifically entropy and fractal dimension. According to Shannon [12], the CE measures signal disorder, which is related to colour variation, but no information on pixel spatial arrangement is provided and depicted as the following equation:

$$H = - \sum_{i=1}^N p_i \cdot \log_2(p_i) \quad (1)$$

Where  $p_i$  is the probability of appearance of pixel value  $i$  in the image and  $N$  the amount of possible pixel values. Besides that, according to Nicolae and Ivanovici [13], many different entropy types and optimised versions have emerged in recent years, each with its own set of advantages, such as multi-scale entropy, cross entropy, fuzzy entropy, and many more when considering spatial information, with additional applications in the biomedical imaging domain.

According to Nicolae and Ivanovici [13], fractal dimension is the most representative measure for expressing the fractal geometry of colour texture images. The fractal dimension expresses texture variations and irregularities in relation to self-similar regions observed across different size scales. Table 1 shows the entropy and fractal values for each image in the Grabcut dataset.

Existing work [14] distinguishes between interactive and semi-automatic segmentation by involving the user in both the initialization and post-processing stages of the segmentation process iteratively, whereas semi-automatic segmentation only involves the user in the initialization stage. This study combines the two terms and defines interactive segmentation as any segmentation that

requires user input. This study, on the other hand, will concentrate on the involvement of user input during the initialization stage.

Various input types are used in interactive segmentation to provide information about the background and object of interest. Some examples of these input formats are as follows:

- i. Strokes [15-17]: The user must apply stroke(s) to the image's object of interest and background.
- ii. Seed point [18-20]: The seed points must be placed on the image's background and object of interest by the user.
- iii. Bounding box [21-23]: The user must position the bounding box around the object of interest within the image.

**Table 1**

Shows entropy and fractal values for each image in the Grabcut dataset

Image	Entropy	Fractal	Image	Entropy	Fractal
106024	7.513	2.438	bush	7.702	2.602
124084	6.914	2.188	ceramic	6.613	2.405
153077	6.842	2.342	cross	7.126	2.499
153093	7.376	2.475	doll	7.252	2.606
181079	7.343	2.606	elefant	6.572	2.535
189080	7.439	2.543	flower	7.525	2.589
208001	7.275	2.874	fullmoon	0.906	2.159
209070	7.506	2.825	grave	7.045	2.902
21077	7.215	2.463	llama	7.014	2.715
227092	6.719	2.661	memorial	6.740	2.720
24077	7.644	1.713	music	7.433	2.828
271008	7.253	2.652	person1	7.483	2.764
304074	7.553	2.782	person2	7.625	2.720
326038	7.178	2.999	person3	7.331	2.656
37073	6.111	2.496	person4	7.628	2.650
376043	7.352	2.786	person5	6.462	2.765
388016	7.108	2.658	person6	7.443	2.546
65019	7.327	2.051	person7	7.557	2.670
69020	6.971	2.887	person8	7.470	2.785
86016	7.373	2.840	scissors	7.054	2.950
banana1	6.277	2.636	sheep	6.545	2.992
banana2	7.026	2.913	stone1	5.554	2.571
banana3	7.133	2.432	stone2	5.554	2.571
book	6.354	2.985	teddy	5.989	2.388
bool	7.218	2.617	tennis	7.427	2.547

In the previous study [7], it was determined that achieving an optimal result in interactive image segmentation can be accomplished by using a bounding box with three strokes. Building upon this insight, our study extends the approach by employing a bounding box as the background and strokes as the foreground in the segmentation process. The number of strokes used is adaptively determined based on the complexity of the images.

To account for image complexity, we introduce a dynamic stroke allocation strategy. Specifically, we consider the fractal value and entropy value as indicators of complexity. For instance, when the fractal value falls below 1.75, we allocate two strokes, while values exceeding 2.75 warrant the use of four strokes. Similarly, for the entropy value, if it is below 1, we allocate two strokes, and if it exceeds 6, we increase the number of strokes to five (See Table 2).

**Table 2**

Shows number of strokes corresponding to each level of fractal and entropy complexity

Fractal	Number of strokes	Entropy	Number strokes
1) <1.75	2	<1.00	2
2) 1.75-2.00	2	1.00-2	2
3) 2.01-2.25	3	2.01-3	2
4) 2.26-2.5	3	3.01-4	3
5) 2.51-2.75	3	4.01-5	3
6) >2.75	4	5.01-6	3
		6.01-7	4
		>7.00	4

In addition to the dynamic stroke allocation strategy, our study also assesses the effectiveness of fixed stroke allocation, as outlined in Table 3. Specifically, we evaluate the impact of employing 2, 3, and 4 strokes on two optimum superpixel sizes: 1000 and 2500.

**Table 3**

Shows the testing configuration based on fixed and dynamic strokes allocations

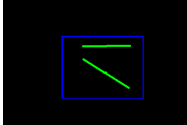
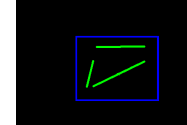
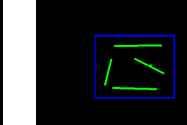
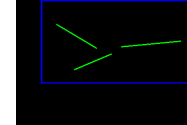
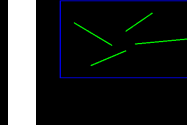
Testing configuration	Foreground(number of strokes)	Background
(a) marker4-2500	4	Bounding box
(b) marker4-1000	4	Bounding box
(c) marker3-2500	3	Bounding box
(d) marker3-1000	3	Bounding box
(e) marker2-2500	2	Bounding box
(f) marker2-1000	2	Bounding box
(g) 2500-entropy	Dynamic	Bounding box
(h) 1000-entropy	Dynamic	Bounding box
(i) 2500-fractal	Dynamic	Bounding box
(j) 1000-fractal	Dynamic	Bounding box

On the other hand, Table 4 provides an overview of the selected test images, including their corresponding ground truth and annotation images, organized based on the number of input strokes and bounding box.

By examining both dynamic and fixed stroke allocation approaches, we aim to compare their respective performances and identify the most suitable strategy for interactive image segmentation. The fixed allocation approach provides a baseline for comparison against the dynamically adjusted strokes, allowing us to evaluate their relative strengths and weaknesses in achieving accurate segmentations.

**Table 4**

Displays the test images, accompanied by their respective ground truth and annotated images

Test image (a)	Ground truth (b)	Marker 2 (c)	Marker 3(d)	Marker 4 (e)
				
				

To quantitatively assess the accuracy of the segmentation results, we utilized widely accepted evaluation metrics [24-26], including the Jaccard index, F1-score, and accuracy.

Error rate (ERR) is the percentage of pixels placed in an incorrect region which is shown as below equation:

$$ERR = 1 - \left( \frac{TP+TN}{TP+TN+TP+FN} \right) \quad (2)$$

However, error rate takes into account the percentage of pixels that accurately map to the background information. As a result, the F-score and Jaccard Index are included.

F-score is equivalent to Dice Coefficient. The F-score is also known as the F1-Score or F-Measure. It is equal to 2 \* the Area of Overlap divided by the total number of pixels in both images.

$$P = \left( \frac{TP}{TP+FP} \right) \quad (3)$$

$$R = \left( \frac{TP}{TP+FN} \right) \quad (4)$$

$$F = 2 * \left( \frac{P*R}{P+R} \right) \quad (5)$$

The Jaccard index, also known as the Intersection over Union (IoU) metric. It is the ratio of the number of pixels that are shared by X and Y to the total number of pixels in X and Y. In this case, X and Y represent the segmented image and ground truth, respectively. The Jaccard index/ IoU formulation is depicted as follow:

$$J/IoU = \left( \frac{TP}{TP+FP+FN} \right) \quad (6)$$

### 3. Results

In this section, we present the results of our experimental study on the relationship between image complexity and the accuracy of interactive image segmentation. We discuss the findings obtained from the various configurations tested and analyse the impact of image complexity measures on the performance of the segmentation algorithm.

Across all the metrics (Jaccard index, F1-score, and accuracy), the results consistently indicate that using 3 or 4 strokes generally leads to better segmentation accuracy compared to using 2 strokes

(See Table 5). This suggests that having more input strokes provides additional information that improves the quality of the segmentation results.

**Table 5**

Presents the segmentation results based on various metrics and testing configurations

Testing configuration	ERR↓	P	R	F↑	J ↑
(a) marker4-2500	<u>0.025</u>	0.950	0.911	0.928	0.869
(b) marker4-1000	<u>0.025</u>	0.944	0.918	<u>0.929</u>	<u>0.873</u>
(c) marker3-2500	0.026	0.946	0.899	0.918	0.858
(d) marker3-1000	<u>0.025</u>	0.943	0.919	<u>0.929</u>	0.872
(e) marker2-2500	0.034	0.946	0.850	0.882	0.810
(f) marker2-1000	0.034	0.947	0.856	0.890	0.816
(g) 2500-entropy	<u>0.025</u>	0.950	0.911	0.928	0.869
(h) 1000-entropy	<u>0.025</u>	0.944	0.918	<u>0.929</u>	<u>0.873</u>
(i) 2500-fractal	0.027	0.950	0.896	0.916	0.855
(j) 1000-fractal	0.027	0.944	0.909	0.923	0.864

The comparison between the configurations with 2500 and 1000 superpixels reveals interesting findings. In general, the configurations with 2500 superpixels achieved slightly higher segmentation accuracy than those with 1000 superpixels. However, the differences were relatively small, indicating that both resolutions can produce acceptable results. This suggests that using a higher number of superpixels does not necessarily guarantee significantly better segmentation accuracy.

The results of the variable stroke configurations based on image complexity measures (entropy and fractal dimension) demonstrate that these approaches can yield competitive segmentation results. The configurations using entropy-based complexity achieved slightly higher scores compared to those using fractal dimension. In terms of error rate, entropy achieved a lower rate (0.025) than fractal dimension (0.027). Similarly, entropy scored higher on the F-score (0.928 vs. 0.916) and the Jaccard index (0.873 vs. 0.864) when using 1000 superpixels. It can conclude that both entropy and fractal dimension effectively capture image complexity with entropy appearing to be slightly more effective in this context.

When comparing the fixed stroke configurations with the variable stroke configurations, it can be observed that the variable stroke configurations achieved similar or slightly better results in terms of segmentation accuracy. This suggests that adapting the number of strokes based on image complexity can potentially enhance the accuracy of the segmentation method.

Table 6 shows the individual result based on 10 testing configurations using Jaccard index matrix. In general, there is consistency in the performance of the different configurations across the images. Some configurations consistently achieve higher Jaccard index scores across multiple images, indicating better segmentation accuracy. However, the results also show some variability in the performance of configurations across different images. For example, in the "bush" image, configurations (a) and (b) (2500 superpixels with 4 and 3 strokes) achieve higher Jaccard index scores compared to configuration (c) (2500 superpixels with 2 strokes). However, in the "ceramic" image, configuration (c) performs better than configurations (a) and (b). Besides that, the variable stroke configurations based on image complexity measures (configurations g, h, i, j) generally perform competitively with the fixed stroke configurations. For example, in the "stone1" and "stone2" images, the variable stroke configurations achieve high Jaccard index scores comparable to the fixed stroke configurations. Lastly, it's worth noting that certain images might present more challenges for segmentation, resulting in lower Jaccard index scores across all configurations. For instance, in the

"music" and "person3" images, all configurations achieve relatively lower scores compared to other images.

**Table 6**

Presents individual results for each of the ten testing configurations, evaluated using the Jaccard Index metric

Testing configuration	(a)	(b)	(c)	(d)	(e)	(f)	(g)	(h)	(i)	(j)
106024	0.802	0.779	0.802	0.779	<u>0.654</u>	<u>0.669</u>	0.802	0.779	0.802	0.779
124084	0.944	0.935	0.944	0.935	0.944	0.935	0.944	0.935	0.944	0.935
153077	<u>0.658</u>	<u>0.626</u>	<u>0.658</u>	<u>0.626</u>	<u>0.659</u>	<u>0.689</u>	<u>0.658</u>	<u>0.626</u>	<u>0.658</u>	<u>0.626</u>
153093	0.769	0.766	0.728	0.791	0.733	0.791	0.769	0.766	0.728	0.791
181079	0.937	0.905	0.961	0.932	0.905	0.932	0.937	0.905	0.961	0.932
189080	0.963	0.963	0.963	0.963	0.963	0.963	0.963	0.963	0.963	0.963
208001	0.935	0.908	0.935	0.908	0.822	0.870	0.935	0.908	0.935	0.908
209070	0.716	0.778	<u>0.694</u>	0.742	<u>0.575</u>	<u>0.593</u>	0.716	0.778	0.716	0.778
21077	0.754	0.873	0.721	0.771	0.854	0.874	0.754	0.873	0.721	0.771
227092	0.944	0.968	0.944	0.968	0.944	0.968	0.944	0.968	0.944	0.968
24077	0.826	0.792	0.801	0.814	<u>0.325</u>	<u>0.520</u>	0.826	0.792	<u>0.325</u>	<u>0.520</u>
271008	0.786	0.779	0.786	0.811	0.764	0.798	0.786	0.779	0.786	0.811
304074	<u>0.646</u>	<u>0.635</u>	<u>0.344</u>	<u>0.634</u>	<u>0.241</u>	<u>0.652</u>	<u>0.646</u>	<u>0.635</u>	<u>0.646</u>	<u>0.635</u>
326038	0.799	0.754	0.801	0.792	0.814	0.750	0.799	0.754	0.799	0.754
37073	0.771	0.828	0.771	0.828	0.741	0.828	0.771	0.828	0.771	0.828
376043	0.887	0.900	0.887	0.900	0.824	0.850	0.887	0.900	0.887	0.900
388016	0.913	0.896	0.913	0.896	0.913	<u>0.449</u>	0.913	0.896	0.913	0.896
65019	0.943	0.951	0.943	0.956	0.943	0.956	0.943	0.951	0.943	0.956
69020	0.868	0.822	0.868	0.822	0.856	0.852	0.868	0.822	0.868	0.822
86016	0.956	0.962	0.956	0.962	0.956	0.962	0.956	0.962	0.956	0.962
banana1	0.759	0.864	0.885	0.864	<u>0.566</u>	<u>0.682</u>	0.759	0.864	0.885	0.864
banana2	0.886	0.758	0.886	0.871	0.886	0.830	0.886	0.758	0.886	0.758
banana3	0.873	0.906	0.903	0.906	0.873	0.905	0.873	0.906	0.903	0.906
book	0.925	0.922	0.925	0.922	0.925	0.919	0.925	0.922	0.925	0.922
bool	0.835	0.800	0.737	0.800	0.635	0.674	0.835	0.800	0.737	0.800
bush	0.783	0.834	<u>0.616</u>	0.834	<u>0.616</u>	0.830	0.783	0.834	<u>0.616</u>	0.834
ceramic	0.911	0.882	0.911	0.776	0.911	<u>0.584</u>	0.911	0.882	0.911	0.776
cross	0.948	0.965	0.948	0.965	0.948	0.965	0.948	0.965	0.948	0.965
doll	0.967	0.956	0.967	0.956	0.967	0.956	0.967	0.956	0.967	0.956
elefant	0.902	0.889	0.902	0.889	0.902	0.889	0.902	0.889	0.902	0.889
flower	0.953	0.956	0.953	0.956	0.953	0.956	0.953	0.956	0.953	0.956
fullmoon	0.938	0.952	0.944	0.952	0.944	0.952	0.944	0.952	0.944	0.952
grave	0.923	0.886	0.923	0.886	0.923	0.886	0.923	0.886	0.923	0.886
llama	0.902	0.912	0.902	0.912	<u>0.472</u>	<u>0.468</u>	0.902	0.912	0.902	0.912
memorial	0.823	0.899	0.823	0.899	0.826	0.899	0.823	0.899	0.823	0.899
music	0.951	0.961	0.951	0.961	0.951	0.961	0.951	0.961	0.951	0.961
person1	0.966	0.954	0.966	0.954	0.966	0.954	0.966	0.954	0.966	0.954
person2	0.938	0.947	0.959	0.947	0.959	0.953	0.938	0.947	0.959	0.947
person3	0.916	0.902	0.916	0.902	0.916	<u>0.578</u>	0.916	0.902	0.916	0.902
person4	0.945	0.906	0.925	0.905	0.893	0.860	0.945	0.906	0.925	0.905
person5	0.857	0.895	0.850	0.892	0.850	0.892	0.857	0.895	0.857	0.895
person6	0.825	0.890	0.782	0.855	<u>0.324</u>	<u>0.409</u>	0.825	0.890	0.782	0.855
person7	0.912	0.888	0.912	0.888	0.912	0.888	0.912	0.888	0.912	0.888
person8	0.926	0.925	0.926	0.925	0.926	0.925	0.926	0.925	0.926	0.925
scissors	<u>0.696</u>	0.708								
sheep	0.894	0.914	0.898	0.914	0.898	0.914	0.894	0.914	0.894	0.905
stone1	0.963	0.954	0.963	0.954	0.963	0.954	0.963	0.954	0.963	0.954
stone2	0.973	0.971	0.973	0.971	0.973	0.971	0.973	0.971	0.973	0.971

---

teddy	0.844	0.927	0.844	0.927	0.844	0.927	0.844	0.927	0.844	0.927
tennis	0.709	<u>0.681</u>	<u>0.675</u>	<u>0.681</u>	<u>0.666</u>	<u>0.617</u>	0.709	<u>0.681</u>	<u>0.675</u>	<u>0.681</u>

---

#### 4. Conclusions

In conclusion, our study investigated the impact of image complexity on the accuracy of interactive image segmentation. By quantifying complexity using entropy and fractal dimension, we observed that image complexity significantly influences segmentation performance. Our dynamic stroke allocation approach, which adapts stroke numbers based on complexity, outperformed fixed allocation. We also explored different configurations, revealing optimal combinations of strokes and superpixel sizes. Our findings emphasize the need to consider image complexity in segmentation algorithms and provide valuable guidance for practitioners. Future research can focus on refining dynamic allocation, exploring additional complexity measures, and applying advanced machine learning techniques to enhance interactive image segmentation in complex scenarios. Overall, our study advances the understanding of image complexity's role and lays the foundation for further advancements in the field.

#### Acknowledgement

The authors would like to thank University of Malaysia Sarawak (UNIMAS) IMPACT Research Grant Scheme (F08/PARTNERS/2119/2021) for the funding.

#### References

- [1] Lim, Sheh Hong, Mohd Azrul Hisham Mohd Adib, Mohd Shafie Abdullah, Nur Hartini Mohd Taib, Radhiana Hassan, and Azian Abd Aziz. "Study of extracted geometry effect on patient-specific cerebral aneurysm model with different threshold coefficient (Cthres)." *CFD Lette*
- [2] Yu, Honghai, and Stefan Winkler. "Image complexity and spatial information." In *2013 Fifth International Workshop on Quality of Multimedia Experience (QoMEX)*, pp. 12-17. IEEE, 2013. <https://doi.org/10.1109/QoMEX.2013.6603194>
- [3] Chai, Soo See, and Kok Luong Goh. "Evaluation of Different User Input Types in Interactive Segmentation." *Journal of Telecommunication, Electronic and Computer Engineering (JTEC)* 9, no. 2-10 (2017): 91-99.
- [4] He, Jia, Chang-Su Kim, C-C. Jay Kuo, Jia He, Chang-Su Kim, and C-C. Jay Kuo. "Interactive image segmentation techniques." *Interactive Segmentation Techniques: Algorithms and Performance Evaluation* (2014): 17-62. [https://doi.org/10.1007/978-981-4451-60-4\\_3](https://doi.org/10.1007/978-981-4451-60-4_3)
- [5] Goh, Kok Luong, Giap Weng Ng, Muzaffar Hamzah, and Soo See Chai. "A Comparative Study of Interactive Segmentation with Different Number of Strokes on Complex Images." *International Journal on Advanced Science, Engineering and Information Technology* 10 (2020): 178-184. <https://doi.org/10.18517/ijaseit.10.1.10240>
- [6] Goh, Kok Luong, Giap Weng Ng, Muzaffar Hamzah, and Soo See Chai. "Sizes of Superpixels and their effect on interactive segmentation." In *2021 IEEE International Conference on Artificial Intelligence in Engineering and Technology (IICAJET)*, pp. 1-5. IEEE, 2021. <https://doi.org/10.1109/IICAJET51634.2021.9573623>
- [7] Goh, Kok Luong, Soo See Chai, Giap Weng Ng, and Muzaffar Hamzah. "Superpixel Sizes using Topology Preserved Regular Superpixel Algorithm and their Impacts on Interactive Segmentation." *International Journal of Advanced Computer Science and Applications* 13, no. 7 (2022). <https://doi.org/10.14569/IJACSA.2022.0130783>
- [8] Goh, Kok Luong, Giap Weng Ng, Muzaffar Hamzah, and Soo See Chai. "Effects of Different Superpixel Algorithms on Interactive Segmentations." *International Journal of Circuits, Systems and Signal Processing* 16 (2022): 1084-1092. <https://doi.org/10.46300/9106.2022.16.131>
- [9] Rother, Carsten, Vladimir Kolmogorov, and Andrew Blake. "' GrabCut' interactive foreground extraction using iterated graph cuts." *ACM transactions on graphics (TOG)* 23, no. 3 (2004): 309-314. <https://doi.org/10.1145/1015706.1015720>
- [10] Ning, Jifeng, Lei Zhang, David Zhang, and Chengke Wu. "Interactive image segmentation by maximal similarity based region merging." *Pattern Recognition* 43, no. 2 (2010): 445-456. <https://doi.org/10.1016/j.patcog.2009.03.004>
- [11] Ren, and Malik. "Learning a classification model for segmentation." In *Proceedings ninth IEEE international conference on computer vision*, pp. 10-17. IEEE, 2003. <https://doi.org/10.1109/ICCV.2003.1238308>

- [12] Shannon, Claude Elwood. "A mathematical theory of communication." *The Bell system technical journal* 27, no. 3 (1948): 379-423. <https://doi.org/10.1002/j.1538-7305.1948.tb01338.x>
- [13] Nicolae, Irina E., and Mihai Ivanovici. "Color texture image complexity—EEG-sensed human brain perception vs. computed measures." *Applied Sciences* 11, no. 9 (2021): 4306. <https://doi.org/10.3390/app11094306>
- [14] Heckel, Frank, Olaf Konrad, Horst Karl Hahn, and Heinz-Otto Peitgen. "Interactive 3D medical image segmentation with energy-minimizing implicit functions." *Computers & Graphics* 35, no. 2 (2011): 275-287. <https://doi.org/10.1016/j.cag.2010.12.006>
- [15] Zhang, Juyong, Jianmin Zheng, and Jianfei Cai. "A diffusion approach to seeded image segmentation." In *2010 IEEE Computer Society Conference on Computer Vision and Pattern Recognition*, pp. 2125-2132. IEEE, 2010. <https://doi.org/10.1109/CVPR.2010.5539891>
- [16] Wang, Tinghuai, Huiling Wang, and Lixin Fan. "A weakly supervised geodesic level set framework for interactive image segmentation." *Neurocomputing* 168 (2015): 55-64. <https://doi.org/10.1016/j.neucom.2015.06.014>
- [17] Ding, Zongyuan, Tao Wang, Quansen Sun, and Hongyuan Wang. "Adaptive fusion with multi-scale features for interactive image segmentation." *Applied Intelligence* 51, no. 8 (2021): 5610-5621. <https://doi.org/10.1007/s10489-020-02114-3>
- [18] Meena, Sachin, Kannappan Palaniappan, and Guna Seetharaman. "User driven sparse point-based image segmentation." In *2016 IEEE International Conference on Image Processing (ICIP)*, pp. 844-848. IEEE, 2016. <https://doi.org/10.1109/ICIP.2016.7532476>
- [19] Xu, Ning, Brian Price, Scott Cohen, Jimei Yang, and Thomas S. Huang. "Deep interactive object selection." In *Proceedings of the IEEE conference on computer vision and pattern recognition*, pp. 373-381. 2016. <https://doi.org/10.1109/CVPR.2016.47>
- [20] Li, Zhuwen, Qifeng Chen, and Vladlen Koltun. "Interactive image segmentation with latent diversity." In *Proceedings of the IEEE Conference on Computer Vision and Pattern Recognition*, pp. 577-585. 2018. <https://doi.org/10.1109/CVPR.2018.00067>
- [21] Wu, Shuqiong, Megumi Nakao, and Tetsuya Matsuda. "SuperCut: Superpixel based foreground extraction with loose bounding boxes in one cutting." *IEEE Signal Processing Letters* 24, no. 12 (2017): 1803-1807. <https://doi.org/10.1109/LSP.2017.2761393>
- [22] Yu, Hongkai, Youjie Zhou, Hui Qian, Min Xian, and Song Wang. "Loosecut: Interactive image segmentation with loosely bounded boxes." In *2017 IEEE International Conference on Image Processing (ICIP)*, pp. 3335-3339. IEEE, 2017. <https://doi.org/10.1109/ICIP.2017.8296900>
- [23] Cheng, Ming-Ming, Victor Adrian Prisacariu, Shuai Zheng, Philip HS Torr, and Carsten Rother. "Densecut: Densely connected crfs for realtime grabcut." In *Computer Graphics Forum*, vol. 34, no. 7, pp. 193-201. 2015. <https://doi.org/10.1111/cgf.12758>
- [24] Taha, Abdel Aziz, and Allan Hanbury. "Metrics for evaluating 3D medical image segmentation: analysis, selection, and tool." *BMC medical imaging* 15 (2015): 1-28. <https://doi.org/10.1186/s12880-015-0068-x>
- [25] Maninis, Kevis-Kokitsi, Sergi Caelles, Jordi Pont-Tuset, and Luc Van Gool. "Deep extreme cut: From extreme points to object segmentation." In *Proceedings of the IEEE conference on computer vision and pattern recognition*, pp. 616-625. 2018. <https://doi.org/10.1109/CVPR.2018.00071>
- [26] Wang, Tao, Zexuan Ji, Quansen Sun, Qiang Chen, Qi Ge, and Jian Yang. "Diffusive likelihood for interactive image segmentation." *Pattern Recognition* 79 (2018): 440-451. <https://doi.org/10.1016/j.patcog.2018.02.023>